Real-time simultaneous temperature and strain measurements at cryogenic temperatures in an optical fiber

Scott Mahar[†a], Jihong Geng[b], Joel Schultz[a], Joseph Minervini[a], Shibin Jiang[b], Peter Titus[a], Makoto Takayasu[a], Chen-yu Gung[a], Wenyan Tian[b], Arturo Chavez-Pirson[b]
[a]Massachusetts Institute of Technology, 77 Massachusetts Ave, Cambridge, MA, USA 02139
[b]NP Photonics, 9030 South Rita Road Suite 120, Tucson, AZ, USA 85747

ABSTRACT

A novel fiber optic sensor has been developed to be used in superconducting magnets for fusion reactors and other large cable-in-conduit superconductor (CICC) magnet applications. These large superconducting magnets need a diagnostic that can measure the temperature and strain throughout the magnet in real-time, which was not possible until now. Simultaneous temperature and strain measurements at cryogenic temperatures have been demonstrated, using spontaneous Brillouin scattering in an optical fiber. Using an extremely narrow (100 Hz) linewidth Brillouin laser with very low noise as a frequency shifted local oscillator, the frequency shift of spontaneous Brillouin scattered light was measured using heterodyne detection. A pulsed laser was used to probe the fiber using Optical Time Domain Reflectometry (OTDR) to determine spatial resolution. The spontaneous Brillouin frequency shift and linewidth as a function of temperature agree with previous literature on stimulated Brillouin scattering data from room temperature down to 4 K. For the first time, the spontaneous Brillouin frequency shift, linewidth, and intensity as a function of strain have been measured down to 4 K. Analyzing the frequency spectrum of the scattered light after an FFT gives the Brillouin frequency shift, linewidth, and intensity of the scattered light. 65,000 pulses, with 53 ns pulse widths, were averaged in under one second, providing a 5 meter spatial resolution along a fiber that was about 100 m long. Measuring these three parameters allow the simultaneous determination of temperature and strain in real-time throughout a fiber with a spatial resolution on the order of several meters.

Keywords: Brillouin, cryogenic, distributed measurement, temperature, strain, superconducting, quench, optical fiber

1. INTRODUCTION

Nuclear fusion reactors are composed of complicated systems that demand both leading edge physics and engineering. Over the last several decades, plasma physics research has brought the idea of a fusion based power plant from small-scale laboratory experiments to the production of megawatts of fusion power. One of the main plasma physics demonstrations is that the confinement of the plasma in a fusion reactor increases with increasing size of the reactor. The International Thermonuclear Experimental Reactor (ITER) is a joint project to build the first power plant size fusion reactor, capable of generating 500 MW of fusion power. Throughout the world, there are many fusion reactors; however, ITER will have twice the diameter of the largest current reactor, which gives it a plasma volume ten times as large.[1] One of the many engineering issues associated with nuclear fusion reactors is the magnet system. Since the plasma needs to be heated to millions of degrees, fusion reactors rely on magnet systems to confine the plasma within its vacuum vessel, so that it does not destroy the walls. A central solenoid magnet is also used to drive current in the plasma, which helps to stabilize the plasma. For ITER to achieve steady state operation using high magnetic field strengths and simultaneously demonstrate satisfactory fusion energy gain, these magnet systems need to be superconducting. Not only do the specifications of the ITER superconducting magnets approach the present limits of superconducting capabilities, but the total stored energy in the magnet set is up to 100 GJ. It is extremely important to have a fast responding system to detect an unstable magnet, so the magnet stored energy can be properly discharged. It is equally important that the detection system can distinguish the magnet signal from background noise in the complicated fusion reactor environment.

[†] smahar@alum.mit.edu; phone 617-324-0731
This work was supported by the U.S. Department of Energy, Grant No. DE-FC02-93ER54186 and No. DE-FG02-07ER84720.

Remote Sensing System Engineering, edited by Philip E. Ardanuy, Jeffery J. Puschell,
Proc. of SPIE Vol. 7087, 70870I, (2008) · 0277-786X/08/$18 · doi: 10.1117/12.791913

One of the most important parts of a superconducting magnet is its quench detection system. When a superconducting magnet quenches, a length of superconducting cable becomes resistive. Unless the current is dumped out of the magnet, it will continue to heat up and could potentially melt the conductor. Most superconducting magnets use voltage taps to measure a voltage drop due to resistance in the magnet. This type of system works well for isolated, small magnets; however, standard voltage taps do not work well for large pulsed magnets, such as the ITER central solenoid.[2] Fusion reactor magnets typically have peak terminal voltages of several kilovolts, which makes the detection of a several millivolt signal very difficult. False positives can cause a magnet to quench when it does not need to, leading to a significant loss of time and money to re-cool and recharge the magnet system; or, in a reactor, to restart a steam turbine.

Fiber optic sensors have a huge advantage over standard sensors in that they are immune to large electromagnetic fields and fluctuations. Inserting a fiber optic cable into a superconducting magnet can provide a distributed temperature measurement throughout the magnet, allowing it to be used as a quench detector. Figure 1 shows how a superconducting cable-in-conduit conductor (CICC) is wound together before being inserted into a square conduit. By winding a fiber in a protective capillary tube in one of the initial triplets, or by running the fiber through the central cooling channel, the fiber would be able to sense a temperature increase rapidly if the magnet begins to quench.

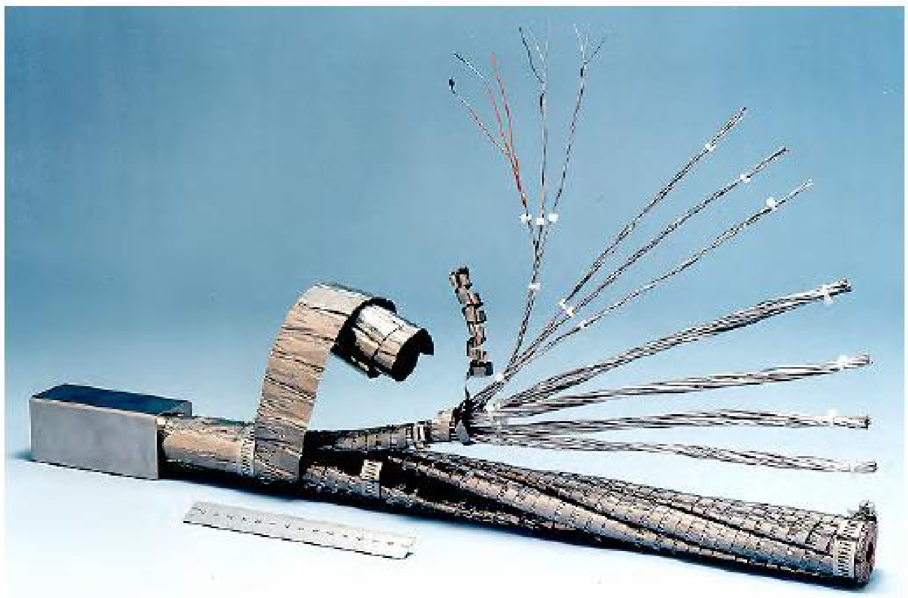

Fig. 1. Short section of a cable-in-conduit conductor partially unwrapped to show the winding pattern. The ITER central solenoid is composed of approximately 36 kilometers of this type of CICC.

A fiber running throughout a superconducting magnet would provide not only a quench protection system, but also a quench locator and a quench propagation diagnostic. Many computer simulations have been created to determine how a quench spreads through a magnet, but the fiber optic sensor presented in this paper could actually measure the quench propagation.[3-5] The spontaneous Brillouin scattering based system can also provide a distributed strain measurement throughout the magnet fabrication and operation, which is also a novel capability in a CICC magnet.

2. EXPERIMENTAL SYSTEM

A single frequency Er-doped fiber laser sends light at 1551 nm through a coupler that splits the light into two different paths, as shown in Figure 2. In the lower path, the light goes through an acousto-optic modulator (AOM), which creates pulses of light of the desired length at the desired rate. The length of this pulse of light in the actual fiber is what determines the spatial resolution of the system. For example, an 80 ns pulse of light corresponds to a spatial resolution of about 8 meters, which is what we chose to use for the strain experiment. After these pulses travel through a circulator to the sensing fiber, which can be hundreds of meters long, the spontaneous Brillouin light is backscattered in the opposite direction.[6]

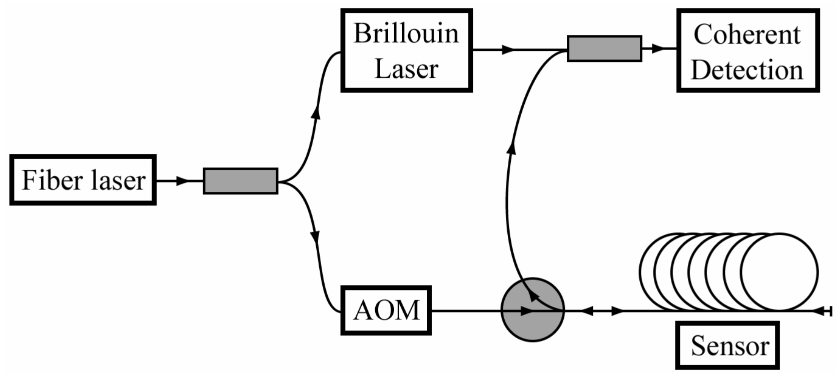

Fig. 2. Schematic diagram of the spontaneous Brillouin scattering system used in these experiments.

The light from the fiber laser going to the upper path is used to pump NP Photonics' Brillouin laser, which is an ultra-narrow linewidth laser (100 Hz).[7] The light leaving the Brillouin laser is combined with the Brillouin backscattered light from the lower path in Figure 2. The Brillouin laser is used as a frequency-shifted local oscillator for the heterodyne detection of the spontaneous Brillouin scattered signal. Since the Brillouin frequency shift is in the 11 GHz range, measuring the frequency of the light within a few MHz is very difficult and expensive. By using a Brillouin laser as a local oscillator, with a frequency nearly 11 GHz lower than that of the fiber laser, the beat signal is heterodyned from the microwave range to the radio frequency range.[8] It is now possible to use a standard detector to measure the frequency shift of the spontaneous Brillouin scattered light.

In order to measure the linewidth of the spontaneous Brillouin scattered light, a MATLAB program was used to take the Fast Fourier Transform (FFT) of the signal. These experiments were done under a Department of Energy Small Business Innovative Research (SBIR) Phase I grant whose main purpose was to show feasibility of this measurement approach. In Phase I, there was insufficient funding and time to develop high speed hardware in addition to the existing system. Instead, the signal was split and run through a General Purpose Interface Bus (GPIB) cable to a second computer, where the signal was recorded. The signal data was run through the MATLAB FFT program to convert the signal data in time to frequency space. Limited by the maximum data transfer speed of the GPIB cable, we were not able to get as many averages of data for the linewidth measurements as we would have liked. A Phase II proposal has been submitted, in which the hardware and support systems for the linewidth measurement will increase the sampling rate by many orders of magnitude.

3. PROOF OF CONCEPT EXPERIMENTS

The experiments discussed in this paper were designed as a proof of concept that a spontaneous Brillouin scattering system can work as a superconducting magnet diagnostic. Other Brillouin scattering systems have worked as distributed temperature and strain sensors; however, these measurements are near or above room temperature.[9,10] In this temperature range, the relation between the temperature and strain and Brillouin scattering parameters are linear.[11-13] At cryogenic temperatures, these relationships are not only non-linear, but also non-monotonic.[14] To complete the proof of concept, Brillouin frequency shift, intensity and linewidth were plotted as functions of temperature and strain from cryogenic temperatures up through room temperature. Using these plots as a multi-dimensional lookup table, the temperature and strain can be determined based on the measured frequency shift, intensity, and linewidth of the spontaneous Brillouin scattered light.

3.1 Temperature experiment

The main goal of the temperature experiment was to characterize the effect of temperature on the spontaneous Brillouin scattering in optical fibers at cryogenic temperatures. One of the most important factors in the design of this experiment was that the fiber needed to be at a uniform temperature during data acquisition. This was confirmed using several gold-chromega thermocouples and a silicone diode. The fiber was wound loosely in a channel cut into an aluminum disk. Including the aluminum lid, the disk was 1 inch thick and 4 inches in diameter, and the fiber channel had an average diameter of 3 inches, as shown in Figure 3. Constantan wire was wound non-inductively on the top and bottom of the disk to act as a heater in order to incrementally increase the temperature.

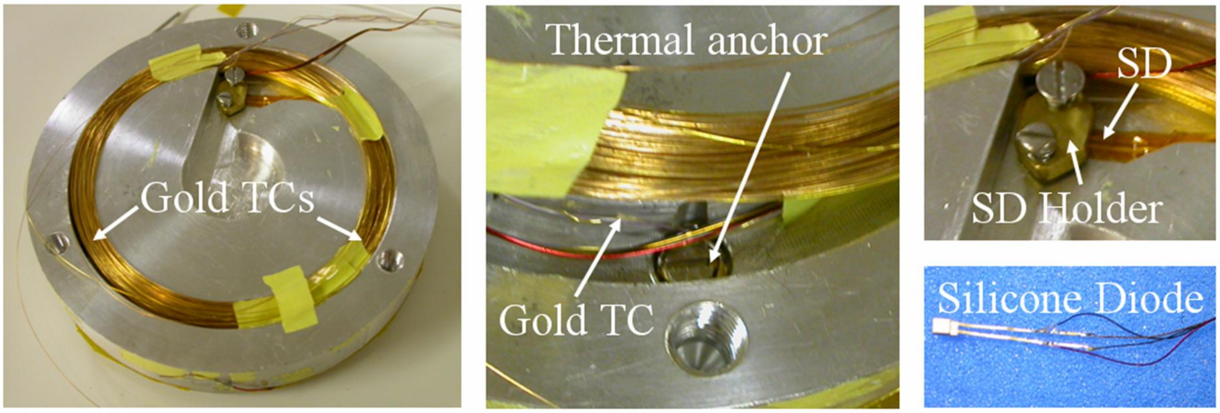

Fig. 3. Location of the thermocouples and silicone diode relative to the coiled fiber for the temperature experiment.

The frequency shift, linewidth, and power were recorded at many different temperatures from 4 K to room temperature. The frequency shift and linewidth data agree qualitatively with data from other experiments, as shown in Figure 4.[14] A quantitative agreement was not expected for two reasons: 1) our system measured the spontaneous Brillouin scattered light, while Thévenaz's system measured the stimulated Brillouin scattered light, and 2) Thévenaz used standard single mode fiber, whereas we used metal coated single mode fibers with different properties due to the coatings. As previously discussed, our system measures the relative frequency shift with respect to the local Brillouin laser oscillator, which was set at roughly 11 GHz less than the pulse laser. In order to compare our data to Thévenaz's data, 11 GHz was subtracted from his frequency shift data.

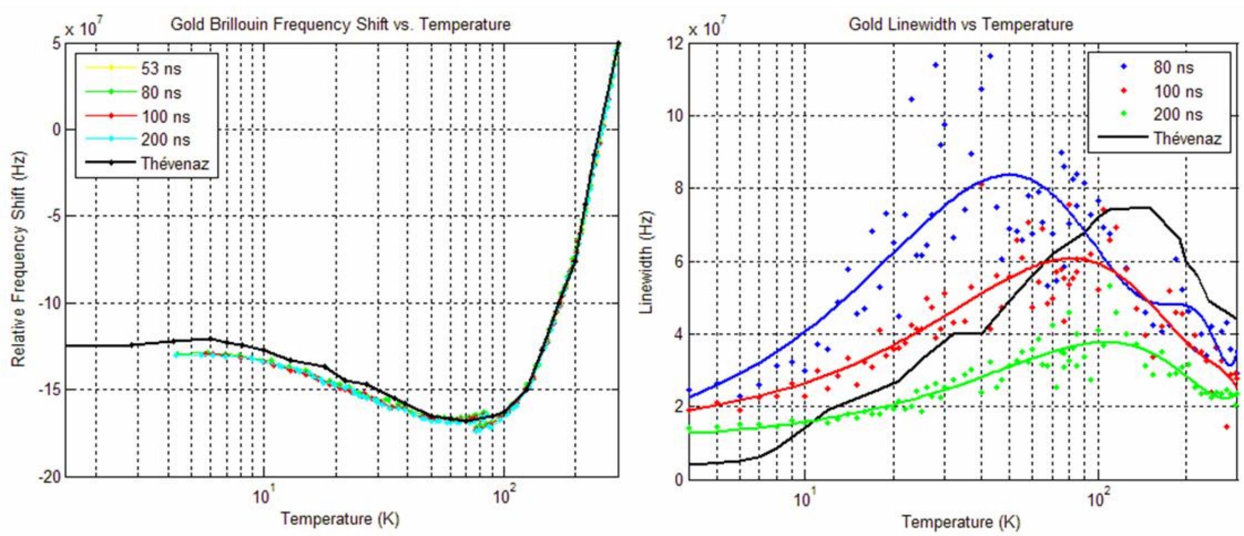

Fig. 4. The relative frequency shift and linewidth as a function of temperature from new experiments (color), compared to Thévenaz (black).

As expected, the frequency shift is not a function of pulse length; however, the linewidth is a function of pulse length. The linewidth data is more scattered than the frequency shift data, since it is derived from only 230 averages of the FFT data, compared to the 65,000 averages that were used for the frequency shift data. This scattering of the data is not a physical phenomenon, but results from the inadequate sampling rate in the linewidth DAQ system. This will be addressed in the Phase II program. Using the FFT data, the relative frequency shifts and intensities at different temperatures were also calculated. This data was compared to the frequency shift and linewidth data shown in Figure 4, and matches extremely well.[15]

On the first day of the experiment, liquid helium was used to generate temperatures from 4 K to 85 K. The probe was removed and warmed up to room temperature overnight, and then liquid nitrogen was used the second day for temperatures from 77 K to room temperature. Figure 4 shows that these two frequency shift data paths are discontinuous, which is due to a change in the fiber properties. The metal coating is applied during the fiber drawing process, which leads to stresses as the fiber cures. The thermal cycle to 4 K and back to room temperature actually cold-worked the fiber, which relieved some of the stresses in the fiber due to the drawing process. This does not eliminate metal coated fibers as potential cryogenic sensors, it simply means that metal coated fibers must be temperature-cycled before they are calibrated as a sensor.

3.2 Strain experiment

Prior to this experiment, there was no data available regarding the effects of strain on the frequency shift, intensity and linewidth of Brillouin scattered light at cryogenic temperatures. Since the best theoretical spatial resolution is on the order of meters, the experiment needs to uniformly strain several times that length of a fiber. Uniformly straining tens of meters of fiber is not too difficult at room temperature, but when it has to be done in liquid helium most of the commonly used straining systems are no longer feasible. In order to map the effect of strain on the Brillouin scattering parameters as a function of temperature as well, the probe also had to be able to control the temperature of the sample fiber.

As in the temperature experiment, it is important that the sample fiber is at a uniform temperature. Liquid helium boiling in a cryogenic experiment will lead to vertical temperature gradients; therefore, the sample fiber should be at as uniform a height as possible. The obvious solution to this problem is to wrap the fibers horizontally around a probe that can expand radially. Since the expected operating strain for ITER magnets is around 2000 $\mu\varepsilon$, and fibers can survive about 10,000 $\mu\varepsilon$ at room temperature, we decided to strain our fibers to around 3500 $\mu\varepsilon$.[16] While this is a relatively small strain, it is higher than the yield strain in most metals, especially in liquid helium which reduces the ductility of most metals. We designed a probe based on the radial expansion of two cone-shaped disks when they are pushed together. The disks were made of a titanium-aluminum-vanadium alloy, Ti-6Al-4V, which has the best cryogenic properties for our experiment.[17] Fingers were cut into the disks which were designed to survive the expected stresses, and also to not buckle under the expected loads. When compressed, these fingers radially expanded a steel cylinder which was sliced into 20 pieces, as shown in Figure 5.

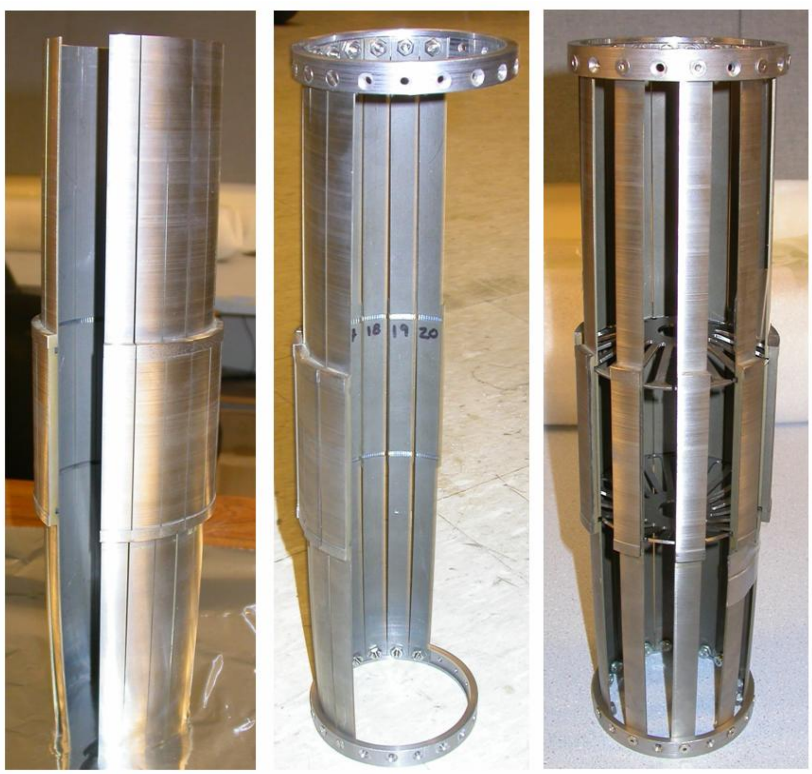

Fig. 5. Pictures of the strain probe: machined and electric discharge machined (EDM) cylinder (left), view of the cylinder's inside grooves and holders (middle), probe with a few sections removed to see the titanium disks (right).

Using a threaded rod with 40 threads per inch, the two disks were forced together in a controlled fashion; however, estimating the actual strain applied is extremely difficult. Due to the thermal expansions of the different types of materials used, as well as the changing level of liquid helium throughout the experiment, an exact correlation between the number of turns and strain applied is not possible. Fiber strain gauges were utilized in order to measure the exact strains felt by the sample fiber. Fiber Bragg Gratings (FBGs) are commonly used as strain gauges, but they are not calibrated at cryogenic temperatures. In order to use FBGs as strain gauges at the cryogenic temperatures in our experiments, we first ran a calibration experiment.[15] Three FBGs placed at the bottom, middle, and top of the sample fiber area were used to ensure that each section was expanding uniformly. The location of these FBGs relative to the sample fibers, as well as the locations of the thermocouples and silicone diode can be seen in Figure 6.

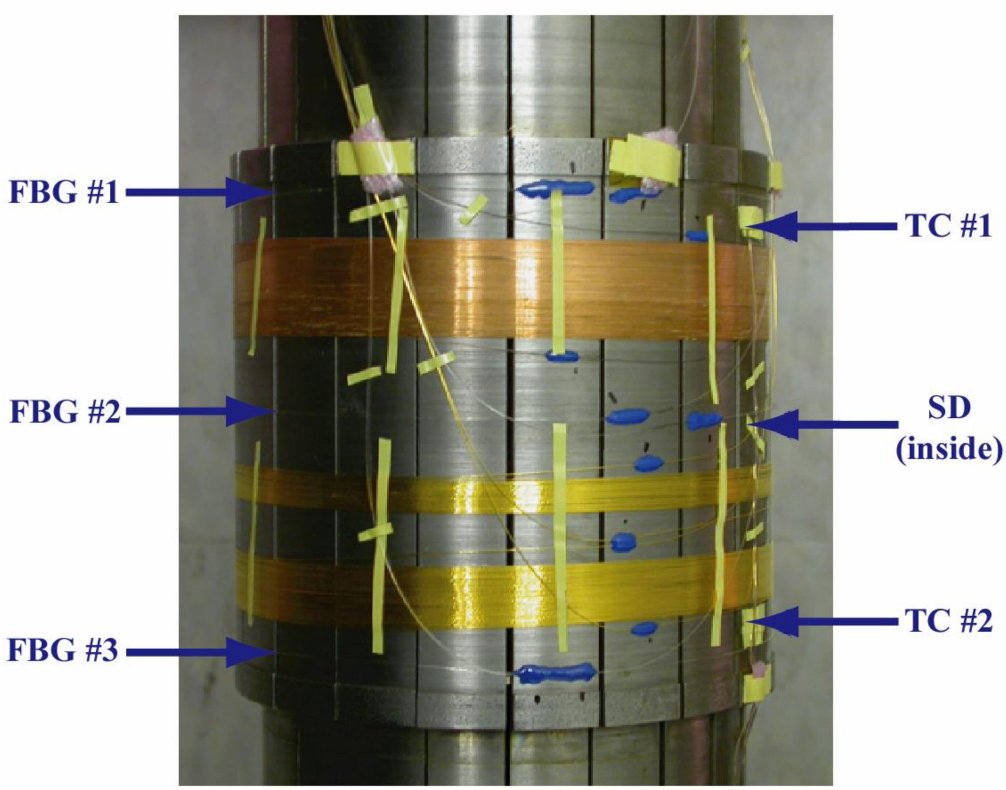

Fig. 6. Picture of the strain probe after the sample fibers have been epoxied into place. The locations of the thermocouples and silicone diode are shown on the right, and the locations of the FBG strain gauges are shown on the left.

A temperature controller was used in conjunction with the silicone diode to heat the fibers to a desired temperature, at which point the fibers were strained to around 3500 με, taking data throughout the strain run. This was done at many different temperatures from 4 K to room temperature to get a good sample of temperature-strain space. By making these measurements over a broad range of temperatures and strains, the experiment allowed mapping of the frequency shift, intensity, and linewidth surfaces as functions of temperature and strain. The following figures include the raw data to visually show how well the surface fit the data.

Throughout the temperature and strain range of our experiment (0-3500 με and 4-300 K), the frequency shift of the spontaneous Brillouin scattered light increased quadratically with increasing strain. A three-dimensional surface was fitted to the data from the strain runs at different temperatures, as shown in Figure 7.

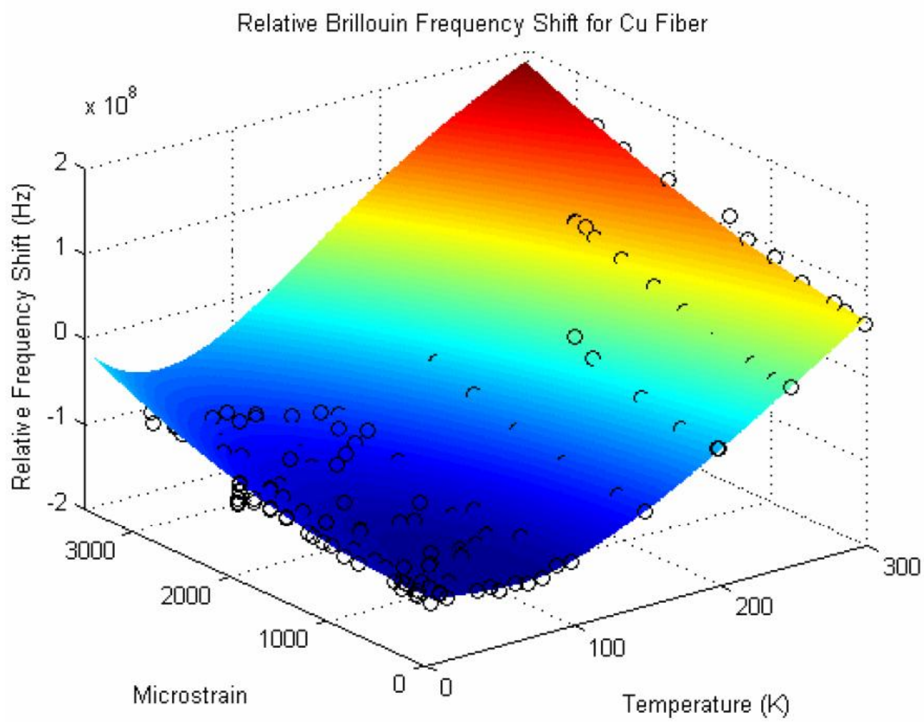

Fig. 7. Surface showing the relative frequency shift as a function of temperature and strain fitted to the experimental data.

The intensity of the Brillouin scattered light was also measured throughout the ranges of temperature and strain. In general, the intensity decreased linearly with increasing strain, as seen in Figure 8.

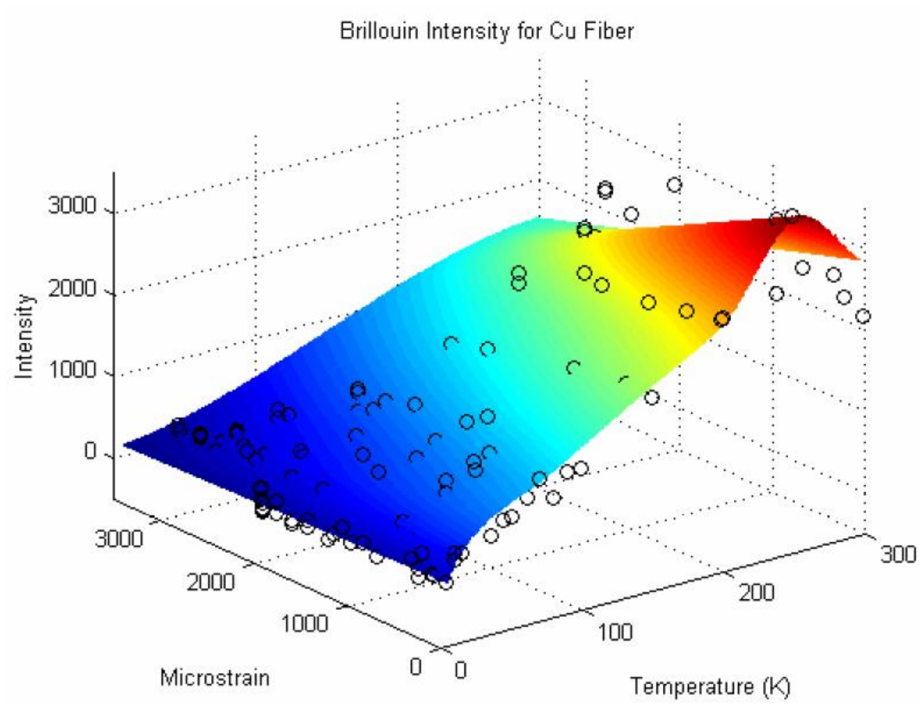

Fig. 8. Surface showing the intensity of the Brillouin scattered light as a function of temperature and strain fitted to the experimental data.

Analysis of the signal data in frequency space revealed that increasing the strain generally increased the linewidth of the Brillouin scattered light, as seen in Figure 9.

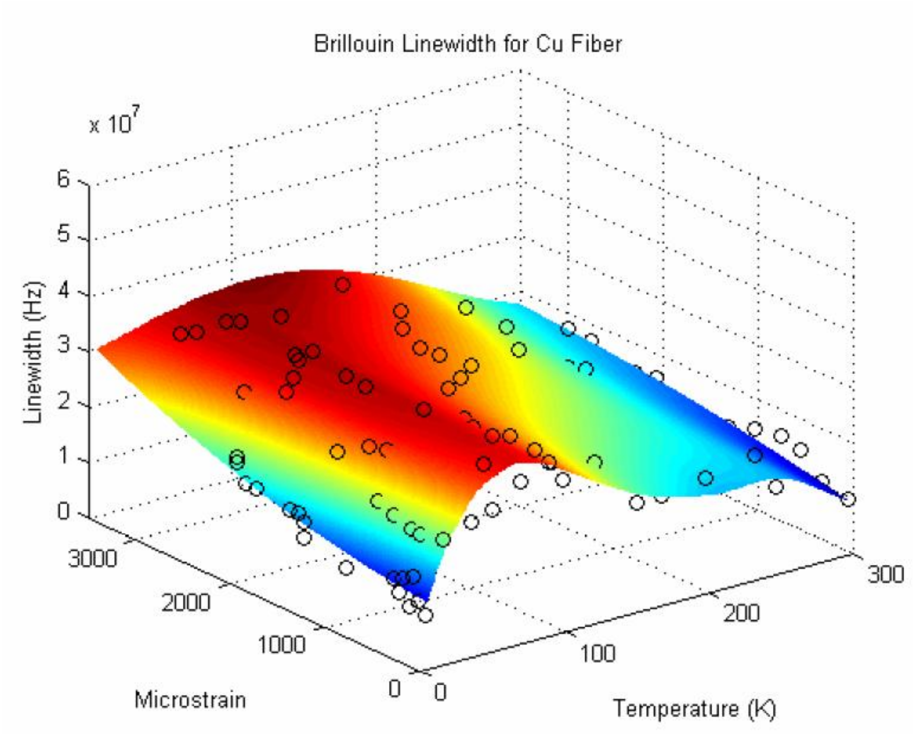

Fig. 9. Surface showing the linewidth of the Brillouin scattered light as a function of temperature and strain fitted to the experimental data.

Despite the small number of averages, leading to poor statistical data for the linewidth calculations, the general shape of the surface can still be plotted. In order to use our system as an actual diagnostic, these surfaces have to be mapped out much more precisely; however, for a proof of concept experiment, the general shapes of the surfaces are all that is needed.

4. SIMULTANEOUS TEMPERATURE AND STRAIN CALCULATIONS

The goal of this system is to be able to measure the spatially resolved temperature and strain throughout the length of the fiber sensor. Using OTDR we can separate measurements and provide spatial resolution. The three-dimensional surfaces shown in Figures 7-9 allow us to calculate unique values of temperature and strain, according to the spatially resolved data. For most of the strain-temperature range we are interested in for use with superconducting magnets, only the frequency shift and intensity are needed. However, there are certain times when the linewidth is also needed to uniquely determine both the temperature and strain.

4.1 Using only frequency shift and intensity

Determining the temperature and strain from only the measured frequency shift and intensity data is possible at room temperature, since both frequency shift and intensity are individually linear with respect to temperature and strain. Since these functions become non-monotonic at cryogenic temperatures, there will be certain regions of temperature and strain that cannot be distinguished, having two or even three values. Using Figures 7 and 8, we can calculate the temperature and strain based on a simulated measurement. Assuming that the system measures a relative Brillouin frequency shift of -100 MHz and an intensity of 1000, we can look at the set of possible temperatures and strains as shown in Figure 10.

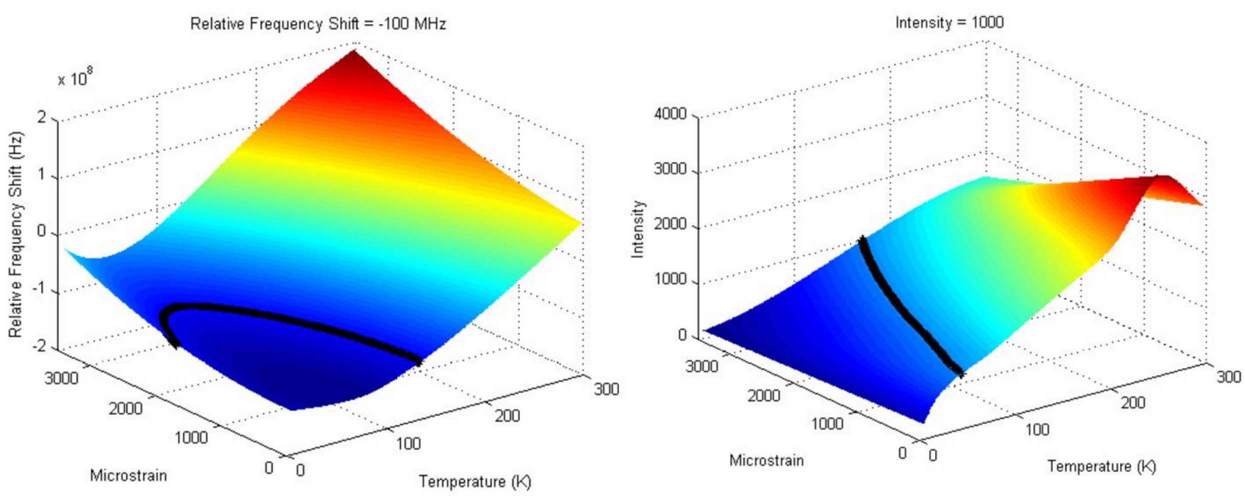

Fig. 10. The temperature and strain data sets (black) are found by taking a slice through the surfaces at the measured value.

The measured temperature and strain are found at the intersection of these two data sets. These data sets, the thicker lines in Figure 11, show that the temperature and strain corresponding to the measured frequency shift and intensity are 95 K and 1900 με, respectively.

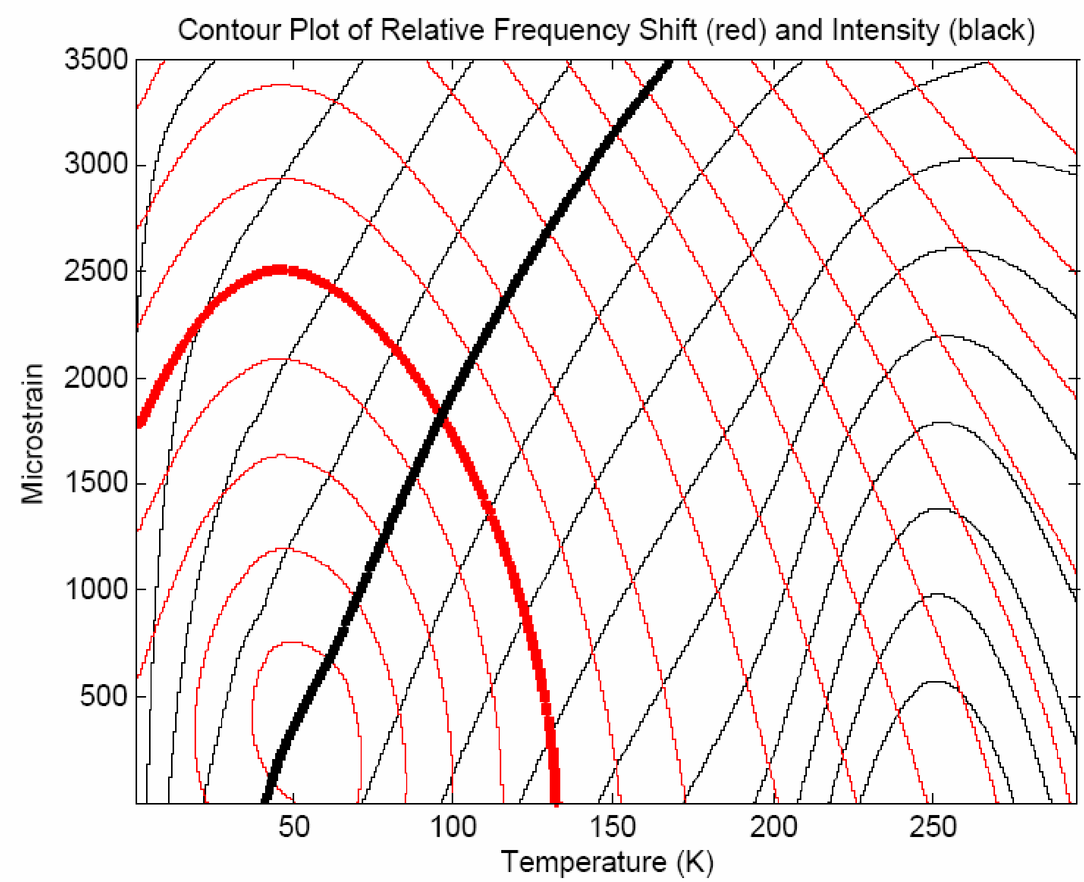

Fig. 11. Contour plot of the relative frequency shift and intensity showing that these two measurements alone can usually provide a unique temperature and strain measurement. The thicker lines are the data sets from the example measurements of -100 MHz and an intensity of 1000 give a temperature of 95 K and a strain of 1900 με.

Since the frequency shift and intensity are both non-monotonic with respect to temperature and strain, a third measurement is required to determine the temperature and strain over the entire range. Fortunately, the non-monotonic parts of the frequency shift and of the intensity occur in different regions of strain-temperature space, as seen in Figure 11. This allows the unique determination of the temperature and strain over most of the plotted range.

4.2 Using frequency shift, intensity, and linewidth

There are certain times when the frequency shift and intensity are not enough to uniquely determine the temperature and strain, which is when the third parameter (linewidth) is needed. If the data sets of temperature and strain from the frequency shift and intensity measurements cross more than once or if they are parallel, the linewidth is needed to uniquely determine the temperature and strain. Using the surfaces generated from the signal data in frequency space, another example measurement can be generated. Assuming that a relative frequency shift of -135 MHz was measured, along with an intensity of 1000, the temperature and strain can not be uniquely determined. The measurement could be 60 K and 700 με, or it could be 45 K and 100 με. Assuming that we also measured a linewidth of 30 MHz, we can determine that the temperature is 45 K and that the strain is then 100 με, as shown in Figure 12.

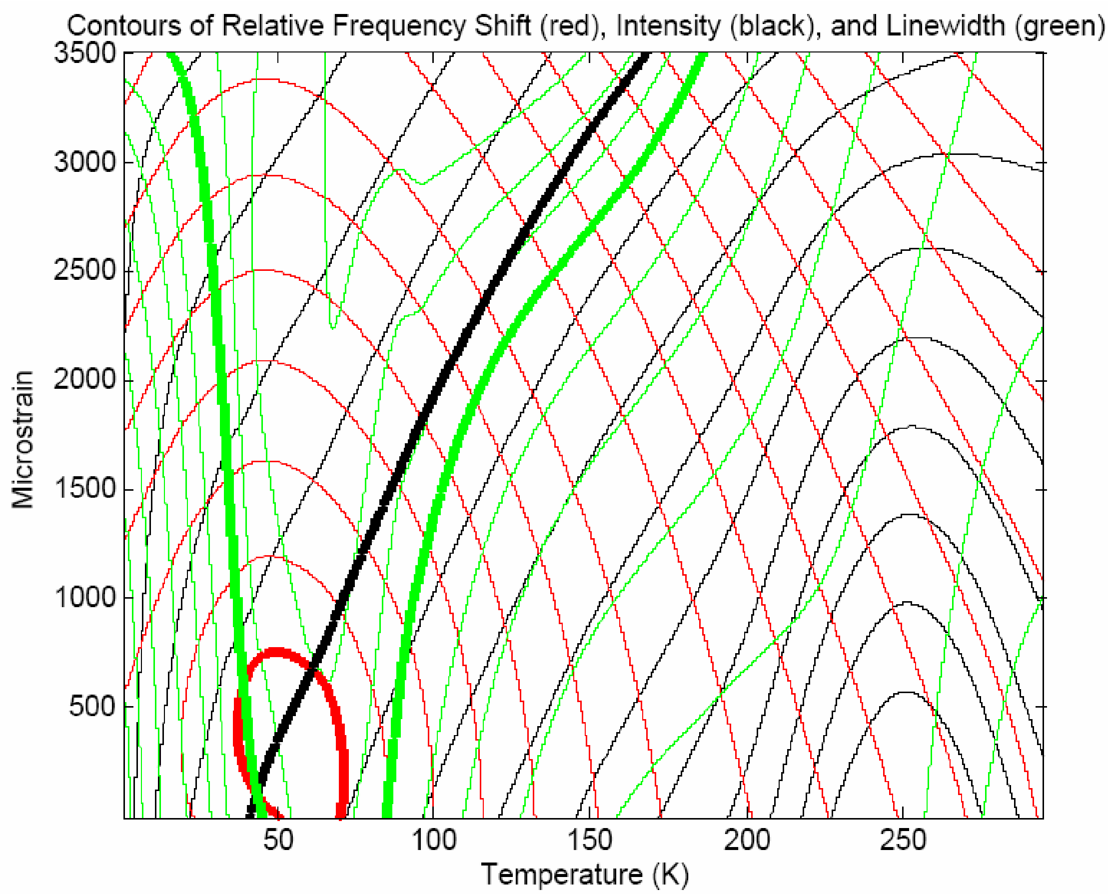

Fig. 12. Contour plots of the relative frequency shift, intensity, and linewidth provide a unique temperature and strain. For the given example measurements, the frequency shift and intensity provide two potential temperatures and strain, but by also using the linewidth measurement, the correct temperature and strain is found.

Figure 12 also shows that the temperature and strain can be uniquely determined throughout the temperature and strain space plotted. In the regions where two of the three parameters are parallel, the third is not. Moreover, the third parameter only intersects this parallel zone once, which allows it to distinguish the appropriate temperature and strain.

4.3 Accuracy of the measurements

The accuracy of the temperature and strain measurement is ultimately dependant the accuracy of the calibration plot, the temperature, and sometimes the strain. While the relation between the accuracy of the measurement and the accuracy of the calibration plot is obvious, the relation between the accuracy of the measurement and the temperature and strain is not as obvious. Since the accuracy of the measurement equipment is constant throughout the temperature range, the error from the DAQ is constant. Taking the DAQ error as a constant, the accuracy of a measurement is dependent on the slope of the calibration curve. For example ± 1 MHz in a region where the frequency shift vs. temperature has a small slope will lead to worse accuracy than a region where the slope is large.

In our system, the error in the frequency shift measurement comes mainly from the frequency counter, which is accurate to less than 1 MHz. Under 12 K (and from 55 K to 65 K), 1 MHz corresponds to about 6 degrees of uncertainty. From about 12 K to 45 K, 1 MHz corresponds to about 2 degrees, and above 70 K, this gives to only 1 degree uncertainty. The accuracy of the frequency shift is also a function of strain since the frequency shift is a quadratic function of strain. Since the effects of strain on the intensity and linewidth are linear, the accuracy of the intensity and linewidth will not be a function of strain. The error for the intensity measurements is on the order of a few percent of the measured value, which is only a degree or two for temperatures below 250 K and above 275 K. Between 250 K and 275 K, the intensity as a function of temperature levels out, increasing the uncertainty to about 10 degrees, but this is not an interesting temperature range for superconducting magnets. Since the statistical FFT data was poor, the accuracy of the linewidth calculations was not calculated, although the data was good enough to determine the general surface of the linewidth in temperature and strain space. For a more detailed discussion of the errors and accuracy of our system, see Reference 15.

Looking at Figures 7-9 it is apparent that regions where the slope is flat in one or even two of the Brillouin scattering parameters, luckily the slope in the other parameter is not flat. For example, at temperatures below 15 K, where the frequency shift slope is flat leading to bad accuracy, the slope of the linewidth is its steepest, which will provide better accuracy. While the linewidth measurement does not provide good accuracy in these experiments, better DAQ hardware in the Phase II experiments will significantly increase the accuracy.

5. CONCLUSIONS AND FUTURE WORK

For the first time, the spontaneous Brillouin frequency shift, intensity, and linewidth as a function of strain have been measured down to 4 K. Using a copper alloy coated fiber, we obtained a spatial resolution of 5 meters at 4 K, and were able to map out the important Brillouin scattering parameters in temperature and strain space. These surfaces proved that a unique temperature and strain can be calculated simply using the frequency shift and intensity for most of the region of interest for superconducting magnets (4-200 K, and 0 – 3500 $\mu\varepsilon$). The linewidth measurement can be used as a check, and is sometimes needed to uniquely determine the temperature and strain in regions where the frequency shift and intensity measurements are not enough.

Since the measurement time is on the order of 0.5 seconds, this system can be used as a quench detection system for large superconducting magnets. The spatial resolution allows the systems not only to locate the origin of the quench, but also to track the temperature changes as the quench spreads. During the heat treatment of a magnet, this system can monitor the temperature throughout the magnet to measure the spatial uniformity of the heat treatment, which has previously been done from the outer surface. Depending on the positioning of the fiber in the winding, this system will also be able to provide the first ever spatially resolved strain measurement in an operating magnet.

In order for this system to be used reliably in an actual magnet system, a more precise calibration experiment needs to be run with an upgraded data acquisition system for the FFT data. There are also several engineering issues that need to be solved, including the extraction of the fiber from pressurized, supercritical helium to a room temperature fiber going to the lasers and DAQ systems.

ACKNOWLEDGMENTS

The authors would like to thank Dave Tracey and the MIT PSFC machine shop technicians for their invaluable help in making the experimental probes. Also, the authors would like to thank Dennis Ryan for all of his help with the experiments at NP Photonics. (Note: Jihong Geng is now with Spectra-Physics/Newport).

REFERENCES

[1] R. Aymar, P. Barabaschi, Y. Shimomura, "The ITER design," Plasma Physics and Controlled Fusion **44,** 519-565 (2002).

[2] J. Schultz, "Superconducting Magnets, Quench Protection," Published in: *Wiley Encyclopedia of Electrical and Electronics Engineering,* J. Webster, **21**. pp. 1-27, New York: John Wiley & Sons, (1999).

[3] L. Bottura, "A Numerical Model for the Simulation of Quench in the ITER Magnets," Journal of Computational Physics, **125**, 26-41 (1996).

[4] A. Shajii, "Theory and Modeling of Quench in Cable-in-Conduit Superconducting Magnets," PFC/RR-94-5, (1994).

[5] J. Feng, "A new thermohydraulic-quench code, SOLXPT3D-Q2," ITER-USMIT-FENG-122007-01, (2007).

[6] M. Alahbabi, Y. Cho, T. Newson, "100 km distributed temperature sensor based on coherent detection of spontaneous Brillouin backscatter," Meas. Sci. Technology **15**, 1544-1547 (2004).

[7] J. Geng, S. Staines, Z. Wang, J. Zong, M. Blake, S. Jiang, "Highly stable low-noise Brillouin fiber laser with ultra-narrow spectral linewidth," IEE Photon Technology Letters **18**, 1813-1815 (2006).

[8] J. Geng, S. Staines, M. Blake, S. Jiang, "Distributed fiber temperature and strain sensor using coherent radio-frequency detection of spontaneous Brillouin scattering," Applied Optics, **46**, No. 23, 5928-5932 (2007).

[9] X. Bao, D. Webb, D. Jackson, "22-km distributed temperature sensor using Brillouin gain in an optical fiber," Optics Letters **18**, 552-554 (1993).

[10] X. Bao, D. Webb, D. Jackson, "Combined distributed temperature and strain sensor based on Brillouin loss in an optical fiber," Optics Letters, **19** No. 2, (1994).

[11] J. Smith, A. Brown, M. DeMerchant, X. Bao, "Simultaneous distributed strain and temperature measurement," Applied Optics, **38** No. 25, 5372-5377 (1999).

[12] X. Bao, Q. Yu, L. Chen, "Simultaneous strain and temperature measurements with polarization-maintaining fibers and their error analysis by use of a distributed Brillouin loss system," Optics Letters, **29** No. 12, (2004).

[13] Y. Li, F. Zhang, T. Yoshino, "Wide-Range Temperature Dependence of Brillouin Shift in a Dispersion-Shifted Fiber and its Annealing Effect," Journal of Lightwave Technology, **21** No. 7 (2003).

[14] L. Thévenaz, A. Fellay, M. Facchini, W. Scandale, M. Nikles, P. Robert, "Brillouin optical fiber sensor for cryogenic thermometry," Proceedings of SPIE, **4694**, (2002).

[15] S. Mahar, "Spontaneous Brillouin Scattering Quench Diagnostics for Large Superconducting Magnets," PhD Thesis, Massachusetts Institute of Technology, (2008).

[16] Fiberguide Industries Data Sheet for Gold Coated Single Mode Fiber. (http://www.fiberguide.com/)

[17] K. Hanby, *Handbook on Materials for Superconducting Machinery*, Columbus, Ohio: MCIC, (1977).